https://doi.org/10.48048/tis.2025.9237

Bioinformatics Examination of Quercetin from *Salacca zalacca* Skin, Fruit, and Seed as a Potent Active Compounds Against Hypercholesterolemia Via PCSK9 Inhibition

Sri Utami[1], Mokhamad Fahmi Rizki Syaban[2], Diana Yuswanti Putri[1], Victor Alvianoes Guterez Hose[1], Husnul Khotimah[3] and Yuyun Yueniwati[4,*]

[1]Master Program in Biomedical Science, Faculty of Medicine, Universitas Brawijaya, Malang 65145, Indonesia
[2]Faculty of Medicine, Universitas Brawijaya, Malang 65145, Indonesia
[3]Department of Pharmacology, Faculty of Medicine, Universitas Brawijaya, Malang 65145, Indonesia
[4]Department of Radiology, Faculty of Medicine, Universitas Brawijaya, Saiful Anwar Hospital Malang, Malang 65111, Indonesia

([*]Corresponding author's e-mail: yuyun@ub.ac.id)

Received: 30 October 2024, Revised: 13 December 2024, Accepted: 20 December 2024, Published: 10 February 2025

Abstract

Hypercholesterolemia is a high-risk factor for cardiovascular disease. The increasing prevalence of hypercholesterolemia necessitates effective therapy. One of the novel targets is proprotein convertase subtilisin/kexin type 9 (PCSK9). However, the high cost of PCSK9 inhibitors limits their availability in low-income and middle-income countries. *Salacca zalacca* (SZ) is an herbal plant with various pharmacological properties, especially cholesterol metabolism. Novel PCSK9 inhibitors from herbal plants may be promising for drug development based on bioinformatic predictive analysis. This study identified SZ compounds as antihypercholesterolemic agents targeting PCSK9 inhibitors and their mechanisms. Pharmacokinetic properties and biological activities were analyzed using the pkCSM and Way2 drug PASS online databases. Molecular docking was performed using PyRx v9.0, PyMOL, and molecular dynamics using the YASARA software. 4-{[(1R)-6-methoxy-1-methyl-1-{2-oxo-2-[(13-thiazol-2-yl)amino]ethyl}-1,2,3,4 tetrahydroiso-quinolin-7-yl]oxy}benzoic acid (PV7) was used as the control. 25 compounds were identified in SZ, and 8 compounds showed good oral bioavailability. Molecular docking showed that quercetin had the strongest binding affinity for PCSK9 (-8.167 ± 0.153 kcal/mol). It was not significantly stronger than the control (-8.067 ± 0.153 kcal/mol) and bound to the same binding residues (TRP 461, ASP 360, SER 462, ARG 357, ARG 458, VAL 333, THR 335, PRO 331, and CYS 358). In addition, molecular dynamic simulation showed a stable interaction between quercetin and PCSK9 with an average RMSD of 3.5 Å. Therefore, quercetin, a phytochemical compound from SZ, is a promising candidate for anti-hypercholesterolemia by targeting PCSK9 inhibitors.

Keywords: PCSK9 inhibitor, Hypercholesterolemia, *Salacca zalacca*, Bioinformatics, Quercetin, Molecular docking, Molecular dynamics

Introduction

Proprotein convertase subtilisin/kexin type 9 (PCSK9) is primarily produced in hepatocytes and functions as a pivotal regulator of cholesterol metabolism by controlling low-density lipoprotein receptors [1]. Strategic treatment is needed along with an increasing prevalence of hypercholesterolemia. PCSK9 inhibitors are promising novel agents and effective treatments for hypercholesterolemia [2,3]. Currently, LDL-lowering drugs targeting PCSK9, such as alirocumab and evolocumab, are 60 % effective in combination with statins; however, their availability is limited and expensive. In the United States, the annual

cost of PCSK9 inhibitors is $5850 per patient, making treatment inaccessible to numerous individuals [4]. This is a major limitation of PCSK9 inhibitors as alternatives to hypercholesterolemia treatment, especially in low- and middle-income countries. Furthermore, alirocumab and evolocumab are approved by the FDA for administration via subcutaneous injections, which may be unpleasant for patients compared to oral drugs [5].

Given these limitations, the development of natural compounds targeting PCSK9 inhibitors has high potential in terms of affordability, availability, and safety profile in drug discovery because of their structural and bioactivity. *Salacca zalacca* (SZ) is one of the tropical fruits indigenous to Indonesia. SZ is a popular dietary herb and has a high flavonoid content, especially quercetin. Previous studies have shown that quercetin may effectively treat atherosclerosis by regulating the expression of PCSK9 [6-9]. A previous study also found that quercetin supplementation reduced atherogenic oxidized LDL (ox-LDL) levels and significantly decreased total cholesterol, LDL, and C-reactive protein [10].

Drug development is complex and expensive. However, advances *in silico* methods using computer simulations and models have revolutionized the development of drugs. These approaches can streamline many steps of the process. By simulating bioinformatics analysis, *in silico* techniques allow researchers to virtually test drug candidates before conducting laboratory and clinical trials [11]. Identifying compounds in SZ that have the best antihypercholesterolemic properties will be useful for drug development. However, no studies have focused on exploring and predicting the potential of quercetin from SZ as a PCSK9 inhibitor using a bioinformatic approach. Therefore, this study explored and predicted the potential of SZ compounds for hypercholesterol treatment by targeting PCSK9 inhibitors, using molecular docking and molecular dynamic simulation. We hope that this study will form the basis for further research on anti-hypercholesterol agents in the future.

Materials and methods

Data mining of phytochemical compounds in *Salacca zalacca*

The phytochemical compounds in SZ have been identified in previous studies [12,13]. The chemical formula, canonical simplified molecular input line entry system (SMILE), 3D structure, and PubChem ID for each compound were downloaded from the PubChem database. All 3D structures of each SZ compound were saved in SDF format for molecular docking analysis.

Drug-likeness, pharmacokinetics, and toxicity prediction

We predicted drug-likeness and performed pharmacokinetic analysis using the pkCSM database (https://biosig.lab.uq.edu.au/pkcsm/). Drug-likeness prediction followed Lipinski's rule of 5 (RoF) criteria [14]. The collected data on RoF included the molecular weight, hydrogen bond acceptor, hydrogen bond donor, partition coefficient, and molecular refractivity. We also evaluated the toxicity class of each compound using ProTox 3.0 prediction (https://tox.charite.de/protox3/index.php?site=home). Compounds that meet the RoF criteria will be advanced to the molecular docking stage for more detailed analysis.

Membrane permeability prediction and biological activity prediction

Membrane permeability was assessed using PerMM (https://permm.phar.umich.edu/) and visualized using ChimeraX (https://www.cgl.ucsf.edu/chimerax) and GraphPad Prism version 10 (https://www.graphpad.com/features). Environmental parameters were selected based on the cell's physiological state, with a pH of 7.4 and a temperature of 310 K. The movement of substances across the plasma membrane was simulated in 3 dimensions [15]. The PerMM method combines the heterogeneous solubility-diffusion theory with an anisotropic solvent model of the lipid bilayer, which is characterized by transbilayer dielectric and hydrogen-bonding parameters. It calculates the membrane binding energies and transfer energy profiles of the permeants, and identifies their optimal positions and conformations during motion along the membrane normal. The membrane-bound state is defined as the conformation

and position with the lowest energy transfer from water [16].

The canonical SMILES for each compound were sourced from PubChem to predict its biological activities. The antihypercholesterolemic activity of SZ was assessed using the WAY2DRUG Prediction of Activity Spectra for Substances (PASS) online tool (http://www.pharmaexpert.ru/passonline/predict.php; accessed March 17, 2024) with its SMILES structure. This tool uses structure-activity relationship (SAR) analysis to compare input compounds with known effective compounds [17,18]. Greater structural similarity leads to higher prediction scores, suggesting that similar structures may exhibit similar bioactivity [18]. Visualization was performed using the GraphPad Prism software version 10 (https://www.graphpad.com/features).

Molecular docking analysis.

Molecular docking simulations were performed using Vina Wizard in PyRx 9.0 (https://pyrx.sourceforge.io/) to predict the interactions between SZ compounds and PCSK9. PCSK9 protein was retrieved from the protein databank (http://www.rcsb.org) with (PDB ID: 6U2N). The quality of the structure of the PCSK9 protein was evaluated using ProCheck on the PDBsum website. Ramachandran website, revealing a most favoured regions [A,B,L] of 89.3 % and a small allowed region of 10.1 %. The dihedral key metrics included a G-factor of -0.25, a covalent radius of 0.33, and an overall G-factor value of 0.11, indicating a good structure quality. The PDB indicates that 6U2N is from organism Homo sapiens, expression system Homo sapiens, with resolution 2.15 Å, R-value of 0.234 (free), R-value of 0.190 (work), R-value of 0.192 (observed), and X-ray crystal structures revealed that these compounds bind to a novel allosteric pocket between the catalytic and C-terminal domains [19]. These results suggested that 6U2N is a suitable candidate for PCSK9 target protein selection. The protein structure was saved in PDB format and prepared using PyMOL software by removing interfering water, adding missing hydrogen atoms, and checking for incomplete residues. The molecules were subsequently converted to the pdbqt format using AutoDock tools [20]. We also used 4-{[(1R)-6-methoxy-1-methyl-1-{2-oxo-2-[(13-thiazol-2-yl)amino]ethyl}-1,2,3,4-tetrahydroisoquinolin-7-yl]oxy}benzoic acid (PV7) as a control based on previous studies [19]. The grid coordinates for specific docking are listed in **Table 1**. Protein-ligand interactions were visualized using BIOVIA Discovery Studio 2019 (https://discover.3ds.com/discovery-studio-visualizer-download).

Table 1 Grid coordinates docking dimension of the study.

	Center			Dimensions (Angstrom)		
Protein Target	**X**	**Y**	**Z**	**Size X (Ao)**	**Size Y (Ao)**	**Size Z (Ao)**
6U2N	−7.760	−24.431	26.230	6.835	6.835	6.835

Molecular dynamics (MD) simulations

Molecular dynamics (MD) simulations were performed using YASARA software with the AMBER14 force field [21]. This process was performed within 100 ns at atinterval of 50,000 fs. The system was also conditioned as closely as possible to the physiological conditions of human cells (temperature at °C, pH 7.4, pressure at 1 atm, and 0.9 % salt content). The macro programs conducted md_run to run the simulations, md_analyze to analyze the root-mean-square deviation (RMSD) values, and md_ analysis to analyze the root-mean-square fluctuation (RMSF) values [22].

Results and discussion

Phytochemical compounds of *Salacca zalacca*

Twenty-five SZ compounds were identified from literature. These compounds are sourced from the skin, fruits, and seeds [12,13]. SZ is a tropical fruit indigenous to Indonesia that is extensively cultivated and consumed in these regions [23,24]. Central Java is the largest salak producer (432,097 tons), equivalent to 38.57 % of the total national salak fruit production per year [25].

Previous studies have shown that SZ contains bioactive compounds such as alkaloids, steroids, triterpenoids, flavonoids, and tannins [26-28]. Its skin also contains quercetin, caffeic acid, chlorogenic acid, ferulic acid, gallic acid, and rosmarinic acid [29,13,30]. The active compounds used in this study are listed in **Table 2**.

Table 2 List of *Salacca zalacca* Compounds.

Compounds ID	Compounds Name	PubChem ID	Molecular Formula	Smile	Structure
SZ 1	Caffeic acid	689043	$C_9H_8O_4$	C1=CC(=C(C=C1C=CC(=O)O)O)O	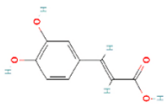
SZ 2	Chlorogenic acid	1794427	$C_{16}H_{18}O_9$	C1C(C(C(CC1(C(=O)O)O)OC(=O)C=CC2=CC(=C(C=C2)O)O)O)O	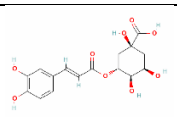
SZ 3	Rutin	5280805	$C_{27}H_{30}O_{16}$	CC1C(C(C(C(O1)OCC2C(C(C(C(O2)OC3=C(OC4=CC(=CC(=C4C3=O)O)O)C5=CC(=C(C=C5)O)O)O)O)O)O)O)O	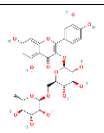
SZ 4	Beta-sitosterone	9801811	$C_{29}H_{48}O$	CCC(CCC(C)C1CCC2C1(CCC3C2CC=C4C3(CCC(=O)C4)C)C)C(C)C	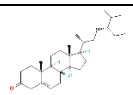
SZ 5	Stigmasterol	5280794	$C_{29}H_{48}O$	CCC(C=CC(C)C1CCC2C1(CCC3C2CC=C4C3(CCC(C4)O)C)C)C(C)C	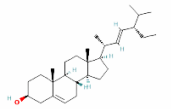
SZ 6	Linoleic acid	5280450	$C_{18}H_{32}O_2$	CCCCCC=CCC=CCCCCCCCC(=O)O	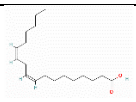
SZ 7	Gallic acid	370	$C_7H_6O_5$	C1=C(C=C(C(=C1O)O)O)C(=O)O	
SZ 8	Ferulic acid	445858	$C_{10}H_{10}O_4$	COC1=C(C=CC(=C1)C=CC(=O)O)O	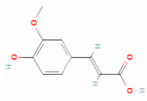
SZ 9	Quercetin	5280343	$C_{15}H_{10}O_7$	C1=CC(=C(C=C1C2=C(C(=O)C3=C(C=C(C=C3O2)O)O)O)O)O	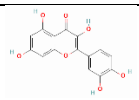
SZ 10	Rosmarinic acid	5281792	$C_{18}H_{16}O_8$	C1=CC(=C(C=C1CC(C(=O)O)OC(=O)C=CC2=CC(=C(C=C2)O)O)O)O	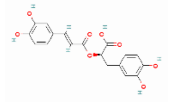
SZ 11	2-methylbutanoic acid	8314	$C_5H_{10}O_2$	CCC(C)C(=O)O	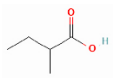
SZ 12	Methyl 3-methylpentanoate	519891	$C_7H_{14}O_2$	CCC(C)CC(=O)OC	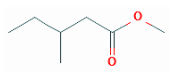
SZ 13	Methyl hexanoate	7824	$C_7H_{14}O_2$	CCCCCC(=O)OC	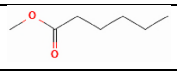
SZ 14	Methyl 3-methyl-2-pentenoate	5362896	$C_7H_{12}O_2$	CCC(=CC(=O)OC)C	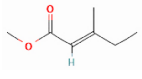
SZ 15	Methyl 3-hydroxy-3-methylpentanoate	13180715	$C_7H_{14}O_3$	CCC(C)(CC(=O)OC)O	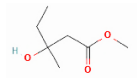

Compounds ID	Compounds Name	PubChem ID	Molecular Formula	Smile	Structure
SZ 16	Furaneol	19309	$C_6H_8O_3$	CC1C(=O)C(=C(O1)C)O	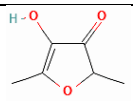
SZ 17	Methyl dihydrojasmonate	102861	$C_{13}H_{22}O_3$	CCCCCC1C(CCC1=O)CC(=O)OC	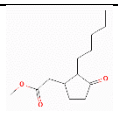
SZ 18	Isoeugenol	853433	$C_{10}H_{12}O_2$	CC=CC1=CC(=C(C=C1)O)OC	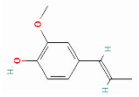
SZ 19	Luteone (Terpenoid)	21601966	$C_{23}H_{36}O_2$	CC(=O)CCC1C(=C)CCC2C1(CCC3C2(CCCC3(C)C)C=O)C	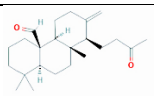
SZ 20	p-cresol	2879	C_7H_8O $CH_3C_6H_4OH$	CC1=CC=C(C=C1)O	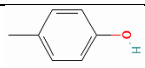
SZ 21	Catechol	289	$C_6H_6O_2$	C1=CC=C(C(=C1)O)O	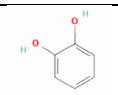
SZ 22	4-methyl catechol	9958	$C_7H_8O_2$	CC1=CC(=C(C=C1)O)O	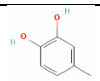
SZ 23	Epicatechin	72276	$C_{15}H_{14}O_6$	C1C(C(OC2=CC(=CC(=C21)O)O)C3=CC(=C(C=C3)O)O)O	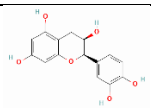
SZ 24	L-DOPA	6047	$C_9H_{11}BO_4$	C1=CC(=C(C=C1CC(C(=O)O)N)O)O	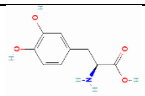
SZ 25	Beta-sitosterol	222284	$C_{29}H_{50}O$	CCC(CCC(C)C1CCC2C1(CCC3C2CC=C4C3(CCC(C4)O)C)C)C(C)C	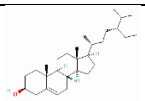

Drug-likeness, bioactivity, pharmacokinetics, toxicity, and membrane permeability of the SZ compounds

This method evaluates drug similarity and determines whether a compound has potential as an oral drug in humans [31]. Oral drug candidates should have a molecular weight below 500 g/mol, lipophilicity (Log P) below 5, hydrogen bond acceptors below 10, hydrogen bond donors below 5, and partition coefficients below 5 [32]. Effective oral drugs also meet the criteria of small molecules and are lipophilic [31]. Based on the drug-likeness screening, for all SZ compounds, 8 compounds fulfilled the ROF criteria, including caffeic acid, ferulic acid, quercetin, rosmarinic acid, methyl dihydrojasmonate, isoeugenol, epicatechin, and L-DOPA, as shown in **Figure 1(A)**. Thus, these compounds are predicted to be potential oral drug candidates. Meanwhile, 17 compounds are not eligible for the RoF criteria, such as beta-sitosterone, stigmasterol, linoleic acid, gallic acid, 2-methylbutanoic acid, methyl 3-methylpentanoate, methyl hexanoate, methyl 3-methyl-2-pentenoate, methyl 3-hydroxy-3-methylpentanoate, furanol, chlorogenic acid, rutin, terpenoid, p-cresol, catechol, 4-methylcatechol, and beta-sitosterol, as shown in **Figure 1(A)**.

The WAY2DRUG PASS online tool was used to determine the biological activities of the compounds based on their structural formulas. This server predicts the activity of each compound by providing a value for probable activity (Pa) and probable inactivity (Pi) [33]. The Pa value indicates the potency of the tested compound, with higher values reflecting greater prediction accuracy [34]. A Pa value between 0.5 and 0.7 indicates a moderate potential for novel pharmacological action. Higher Pa values indicate better accuracy and greater structural similarity [18,35]. We evaluated 8 SZ compounds that have good oral bioavailability with The WAY2DRUG PASS to

determine the bioactivity of each compound. Based on the bioactivity prediction, epicatechin and caffeic acid had higher Pa values (0.63). This was followed by ferulic acid (0.6250), quercetin (0.5160), methyl dihydrojasmonate (0.51), L-dopa (0.0098), isoeugenol (0.0067), and rosmarinic acid (0.0029) (**Figure 1(B)**). These results showed that epicatechin, caffeic acid, ferulic acid, quercetin, and methyl dihydrojasmonate have a moderate probability of anti-hypercholesterolemia activity, suggesting that these compounds may also contribute to cholesterol regulation. Previous studies have shown that epicathechin is significantly decreased total cholesterol, LDL cholesterol, and triglyceride levels while increasing HDL cholesterol [36]. In addition, caffeic acid, ferulic acid, quercetin significantly lowered the plasma lipid and hepatic cholesterol levels [37-39]. In other research, quercetin has the potential to treat metabolic disorders due to its pharmacological properties, including hypoglycemic, hypolipidemic, cardioprotective, anti-inflammatory, anticancer, and hepatoprotective effects [40-44].

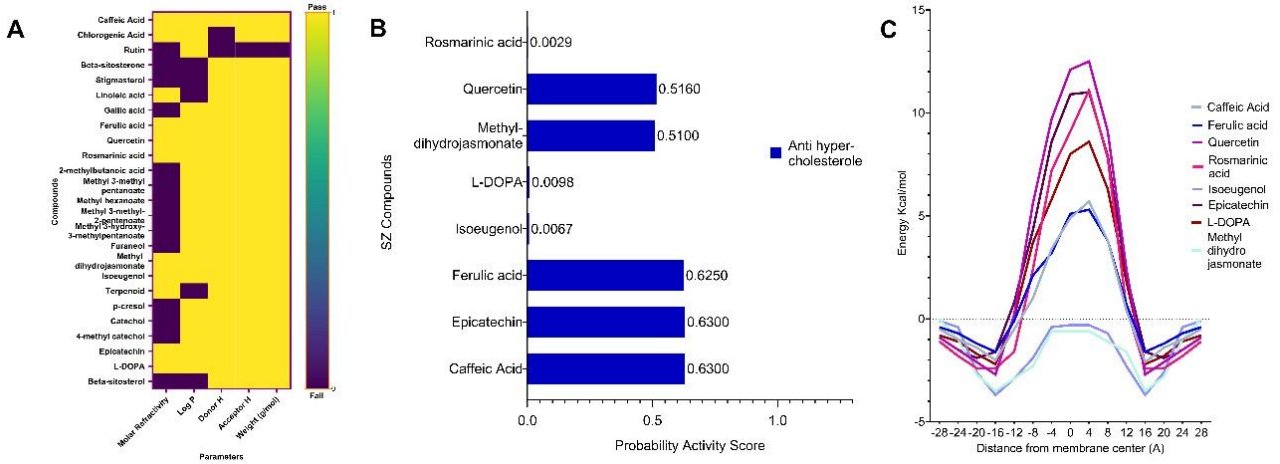

Figure 1 Prediction characteristics of SZ. (A) Rule of 5 (RoF) predictions for SZ compounds. (B) Prediction of biological activity of SZ compounds. (C) Prediction of the membrane permeability of SZ compounds.

The PerMM database analyzes and visualizes the passive translocation of compounds across lipid membranes. This method calculates the total energy of a compound passing through cell membranes [16]. Membrane permeability analysis demonstrated that methyl dihydrojasmonate had the higher permeability, with energy values being −0.6 kcal/mol, respectively (**Figure 1(C)**, **Figure 2**). Followed by isoeugenol (−0.3 kcal/mol), caffeic acid (4.90 kcal/mol), ferulic acid (5.1 kcal/mol), L-Dopa (8.0 kcal/mol), rosmarinic acid (9.1 kcal/mol), epicatechin (10.9 kcal/mol), and quercetin (12.1 kcal/mol). It means that methyl dihydrojasmonate had a greater ability to enter the plasma membrane than other compounds by their conformational changes as they entered the cell membrane. Quercetin has a lower permeability (12.1 kcal/mol) than the others, indicating that it may be difficult and take longer to pass through the acyl chain area. As a result, viable delivery mechanisms, such as liposomes or nanoparticles, are required to make quercetin easily penetrate the lipid acyl chain area of the lipid bilayer [45].

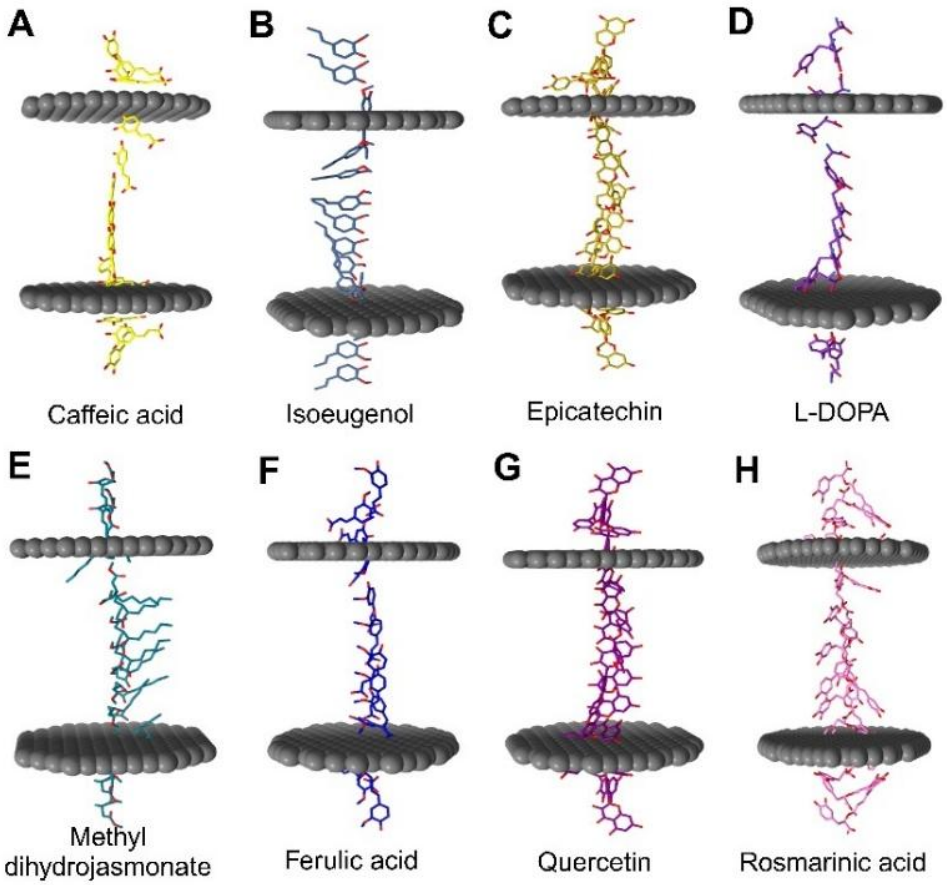

Figure 2 Visualization of membrane permeability of SZ compounds.

ADMET characteristics, including absorption, distribution, metabolism, excretion, and toxicity, play an important role in drug discovery, development, and design strategies [46]. Pharmacokinetic analysis indicated that all 8 compounds had low water solubilities. According to the absorption parameters, caffeic acid, rosmarinic acid, epicatechin, and L-dopa showed moderate intestinal absorption. However, ferulic acid, quercetin, methyl dihydrojasmonate, and isoeugenol show high intestinal absorption. Additionally, all compounds had low blood-brain barrier (BBB) penetration, except isoeugenol, which demonstrated higher permeability.

Furthermore, these 8 compounds were subjected to toxicity screening to identify nontoxic compounds in the human body. According to the Pro-Tox II prediction, L-dopa, isoeugenol, and ferulic acid have class IV toxicity. Caffeic acid, rosmarinic acid, and methyl dihydrojasmonate belong to the toxicity class V. Epicatechin belongs to class VI toxicity. Toxicity categories IV, V, and VI are non-toxic and non-irritating [47]. However, quercetin has class III toxicity, with an LD50 of 159 mg/kg, suggesting that it is more toxic when ingested in amounts exceeding 159 mg/kg body weight, as shown in **Table 3**. The use of quercetin should be seriously considered, because it is slightly harmful but not dangerous when administered orally. Therefore, the use of quercetin at safe doses in experimental studies should be considered.

Table 3 Pharmacokinetic and toxicity computation analysis of *Salacca zalacca* Prediction.

SZ compounds	Pharmacokinetic test*			Toxicity computation analysis**	
	Water solubility	Human intestine absorption ion (HIA)	Penetrate Blood Brain Barrier (BBB)	Predicted LD_{50} (mg/kg)	Toxicity class
Caffeic Acid	Low	Medium	Low	2980	5
Ferulic acid	Low	High	Low	1772	4
Quercetin	Low	High	Low	159	3
Rosmarinic acid	Low	Medium	Low	5000	5
Methyl dihydrojasmonate	Low	High	Low	5000	5
Isoeugenol	Low	High	High	1560	4
Epicatechin	Low	Medium	Low	10000	6
L-DOPA	Low	Medium	Low	1460	4

*pkCSM, **Protox-3.0

Molecular docking

Molecular docking is a computational method for predicting potential drug candidates with strong binding affinity and specificity, such as drug candidates or ligands, and a receptor or target protein [48]. Molecular docking can expedite the identification and optimization of bioactive compounds from natural sources for therapeutic applications. Molecular docking was conducted to determine the interactions between the active constituents of SZ that met the Ro criteria and could be used as drug candidates against PCSK9 with a binding affinity score, as shown in **Figure 3**. To validate the molecular docking protocol, we performed re-docking, as shown in **Figure 3(A)**. Molecular docking results demonstrated that, among the 8 compounds, quercetin had the highest binding affinity for PCSK9. Quercetin could bind more strongly than the control with a binding affinity score of −8.167 ± 0.153 kcal/mol, which is higher than the control with a binding affinity score of −8.067 ± 0.153 kcal/mol, as shown in **Figure 3(B)**. This result aligns with previous studies indicating that quercetin has a higher binding affinity of −8.67 ± 0.009 kcal/mol for bovine serum albumin than for amyloid beta-peptide (1 - 42) (−5.37 ± 0.05 kcal/mol) and 3D amyloid-beta fibers (1 - 42) (−5.93 ± 0.13 kcal/mol), based on molecular docking results [20].

The SZ compounds are highlighted in bold font to indicate their comparable binding and similar interactions with the control, as shown in **Table 4**. In contrast, the other compounds, epicatechin (−7.600 ± 0.2 kcal/mol), rosmarinic acid (−6.967 ± 0.153 kcal/mol), caffeic acid (−6.233 ± 0.208 kcal/mol), L-dopa (−6.233 ± 0.153 kcal/mol), ferulic acid (−6.000 ± 0.100 kcal/mol), isoeugenol (−5.467 ± 0.153 kcal/mol), methyl dihydrojasmonate (−5.333 ± 0.153), as shown in **Figure 3(B)**. The bond scores were below the control (more positive value), indicating lower bond strength [49,50]. Binding energy prediction involves calculating the physicochemical properties of the ligand-receptor complex. A low (negative) energy value suggests a stable complex with a high likelihood of binding interactions [51]. The results of the binding affinity score were analyzed using a one-way ANOVA statistical test, as shown in **Figure 3(B)**.

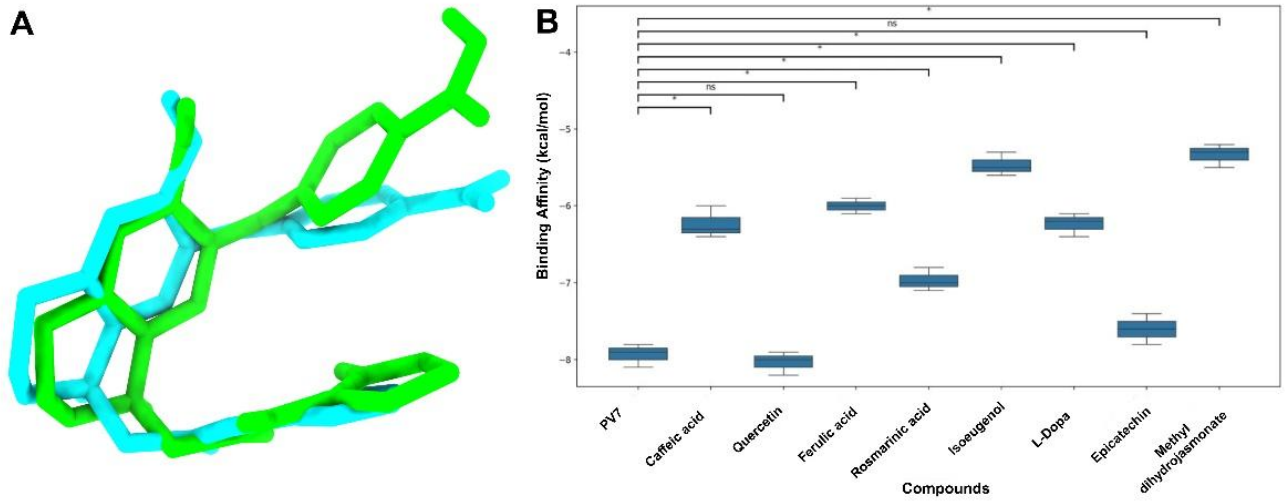

Figure 3 The binding affinity of SZ compounds against PCSK9 from the molecular docking results (A) Re-docking of the native ligand pre- and post-docking. (B) Statistical analysis of the binding affinity scores from the molecular docking results of SZ compounds against PCSK9.

Quercetin appeared to bind to the same binding pocket as the control, as shown in **Figure 4(A)**. Quercetin can bind to PCSK9 via hydrogen bonds at TRP 461, ILE 474, and ASP 360; hydrophobic interactions at residues SER 462, ALA 475, ARG 357, ARG 458, ARG 412, VAL 333, ILE 334, THR 335, and CYS 358; and Pi-alkyl interactions at ARG 476, VAL 460, and PRO 331, as shown in **Figure 4(B)**. Meanwhile, the control (PV7) could bind to PCSK9 via hydrogen bonds at CYS 358, ARG 357, PRO 331, ARG 458, and ARG 476, as well as hydrophobic interactions at VAL 333, SER 329, PRO 478, GLU 332, ASP 360, ARG 412, THR 335, ALA 330, SER 462, TRP 461, VAL 460, and CYS 477, an unfavorable bump at UNK 1, and Pi-Alkyl at ALA 478 residues, as shown in **Figure 4(C)**. Quercetin had the same residues as the control, such as TRP 461, ASP 360, SER 462, ARG 357, ARG 458, VAL 333, THR 335, PRO 331, and CYS 358. This result is consistent with previous studies that showed that PCSK9 contains several critical residues at ASP360, ARG357, ARG458, and ARG476 [19]. Other SZ compounds could also bind to the same binding residue as the control, as shown in **Table 4** and **Figure 4(D)** visualization, as shown in **Figure 5**.

Molecular docking results show that quercetin has the highest binding affinity among the SZ compounds, although it is not significantly different from the control (PV7). Previous studies show that quercetin may effectively treat atherosclerosis by regulating PCSK9 and also reducing levels of atherogenic oxidized LDL (ox-LDL), total cholesterol, LDL, and C-reactive protein [6-10]. Based on the binding affinity results, we procced quercetin to continue the molecular dynamics simulation examination.

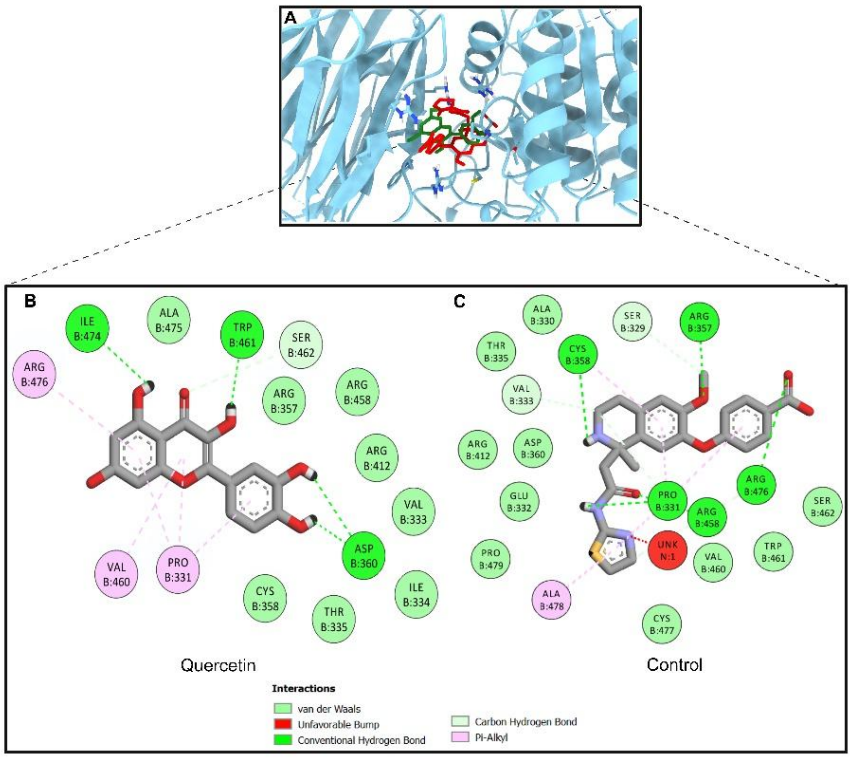

Figure 4 Visualization of quercetin and control (PV7) against PCSK9. (A) Superimposed interactions of quercetin (green) and PV7 (control) (red) with PCSK9 in the same binding pocket. (B) 2D interaction between quercetin and PCSK9. (C) 2D interaction between PV7 (control) and PCSK9.

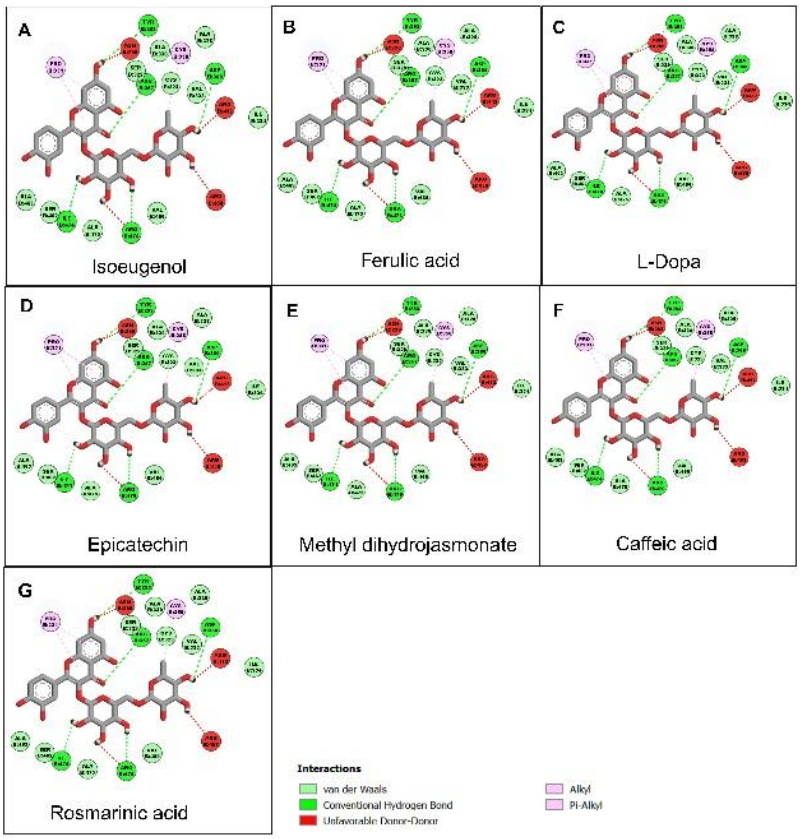

Figure 5 2D visualization of the molecular interactions of the SZ compounds with PCSK9. (A) Isoeugenol (B) Ferulic acid (C) L-dopa (D) Epicatechin (E) Methyl dihydrojasmonate (F) Caffeic acid (G) Rosmarinic acid.

Table 4 Molecular interaction between SZ compounds and PCSK9.

Compounds	Binding affinity (kcal/mol)	Interaction	Amino acid residues
Quercetin	−8.167 ± 0.153	Hydrogen bond	**TRP 461;** ILE 474; **ASP 360.**
		Hydrophobic	**SER 462,** ALA 475; **ARG 357; ARG 458; ARG 412; VAL 333;** ILE 334; **THR 335; CYS 358.** ARG 476; VAL 460; PRO 331.
		Pi-Alkyl	
Control (PV7)	−8.067 ± 0.153	Hydrogen bond	**CYS 358; ARG 357;** PRO 331; **ARG 458;** ARG 476.
		Hydrophobic	**VAL 333;** SER 329, PRO 478; GLU 332; **ASP 360; ARG 412; THR 335;** ALA 330; **SER 462; TRP 461;** VAL 460; CYS 477.
		Unfavorable bump	UNK 1
		Pi-Alkyl	ALA 478
Epicatechin	−7.600 ± 0.2	Hydrogen bond	ASP 360; **ARG 357; TYR 293; ILE 474; ARG 476.**
		Hydrophobic	ALA 330; ALA 328; SER 329; CYS 323; VAL 333; ILE 334; VAL 460; ALA 475; SER 462; ALA 463.
		Alkyl-Pi	CYS 358; PRO 331.
		Unfavorable donor	ARG 458, ARG 412; ASN 298.
Rosmarinic acid	−6.967 ± 0.153	Hydrogen bond	ASP 360; **ARG 357; TYR 293; ILE 474; ARG 476.**
		Hydrophobic	ALA 330; ALA 328; SER 329; CYS 323; VAL 333; ILE 334; VAL 460; ALA 475; SER 462; ALA 463.
		Pi Alkyl	CYS 358; PRO 331.
		Unfavorable donor	ARG 458, ARG 412; ASN 298.
Methyl dihydrojasmoate	−5.333 ± 0.153	Hydrogen bond	ASP 360; **ARG 357; TYR 293; ILE 474; ARG 476.**
		Hydrophobic	ALA 330; ALA 328; SER 329; CYS 323; VAL 333; ILE 334; VAL 460; ALA 475; SER 462; ALA 463.
		Pi Alkyl	CYS 358; PRO 331.
		Unfavorable donor	ARG 458, ARG 412; ASN 298.
Caffeic acid	−6.233 ± 0.208	Hydrogen bond	ASP 360; **ARG 357; TYR 293; ILE 474; ARG 476.**
		Hydrophobic	ALA 330; ALA 328; SER 329; CYS 323; VAL 333; ILE 334; VAL 460; ALA 475; SER 462; ALA 463.

Compounds	Binding affinity (kcal/mol)	Interaction	Amino acid residues
		Alkyl-Pi alkyl	CYS 358; PRO 331.
		Unfavorable donor	ARG 458, ARG 412; ASN 298.
Ferulic acid	−6.000 ± 0.1	Hydrogen bond	ASP 360; **ARG 357; TYR 293; ILE 474; ARG 476.**
		Hydrophobic	ALA 330; ALA 328; SER 329; CYS 323; VAL 333; ILE 334; VAL 460; ALA 475; SER 462; ALA 463.
		Pi alkyl	CYS 358; PRO 331.
		Unfavorable donor	ARG 458, ARG 412; ASN 298.
Isoeugenol	−5.46 ± 0.153	Hydrogen bond	ASP 360; **ARG 357; TYR 293; ILE 474; ARG 476.**
		Hydrophobic	ALA 330; ALA 328; SER 329; CYS 323; VAL 333; ILE 334; VAL 460; ALA 475; SER 462; ALA 463.
		Pi alkyl	CYS 358; PRO 331.
		Unfavorable donor	ARG 458, ARG 412; ASN 298.
L-DOPA	−6.233 ± 0.153	Hydrogen	ASP 360; **ARG 357; TYR 293; ILE 474; ARG 476.**
		Hydrophobic	ALA 330; ALA 328; SER 329; CYS 323; VAL 333; ILE 334; VAL 460; ALA 475; SER 462; ALA 463.
		Alkyl-Pi alkyl	CYS 358; PRO 331.
		Unfavorable donor	ARG 458, ARG 412; ASN 298.

*Residues in bold and underlined indicate the active site residues of the target protein.

Molecular dynamic simulation

Molecular dynamics (MD) simulations were developed to investigate the time evolution of protein conformations and to obtain detailed kinetic and thermodynamic data, including the motion of each atom over time. MD simulations offer large amounts of quantitative data on the structure and dynamics of proteins and peptides [52]. RMSD results showed the stability of the receptor complex to the ligand. The control RMSD results showed a good RMSD value, with an average of 2.76 Å. This indicates that PV7 (control) exhibited strong stability during the simulation process.

The RMSD of quercetin was relatively stable during the first 40 ns of the simulation. Subsequently, a fluctuation in the RMSD value that reached 5.3 Å. This fluctuation gradually decreased with a stable RMSD value of 3.5 Å in the last 50 ns of the simulation, as shown in **Figure 6(A)**. RMSF analysis showed that residue ALA168 has the highest fluctuation, with values of control 8.4 and quercetin 5.2. PCSK9 critical residues, such as ARG357, ASP360, ARG458, and ARG476, have a low RMSF value of less than 3 Å. These results suggest that the active site of PCSK9 retains its stability when it is complexed with quercetin. This indicates that the active site of the receptor is relatively stable with minimal fluctuation and flexibility [53]. Proteins were considered stable in the simulation if their RMSD value was ≤ 3 Å; higher values indicated structural changes. RMSF measures amino acid

fluctuations, with high values indicating instability. Stable RMSD and RMSF values are essential for evaluating protein-ligand binding affinity [53,54].These fluctuations are shown in **Figure 6(B)**.

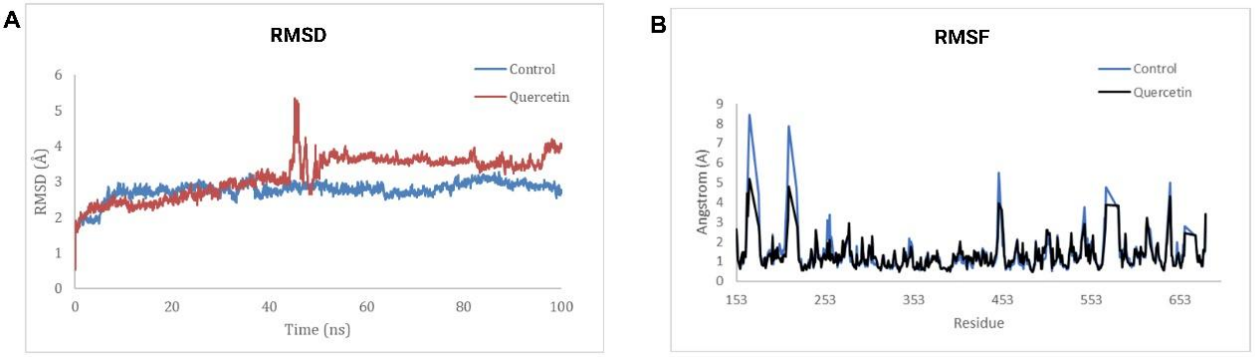

Figure 6 Molecular dynamics simulation of quercetin against PCSK9. (A) Root Mean Square Deviation (RMSD). (B) Root Mean Square Fluctuation (RMSF).

Conclusions

The compounds identified in SZ, particularly quercetin, demonstrated significant potential as PCSK9 inhibitors, offering a natural and possibly more affordable alternative to existing monoclonal antibody therapies. Quercetin has shown stronger, more stable binding to PCSK9 and is the most promising cholesterol-lowering agent against PCSK9 in SZ. Enabling prediction of its inhibitory effect on the activity of these proteins. This study provides a solid foundation for further experimental validation, with the ultimate goal of developing novel, natural therapies for hypercholesterolemia that are both effective and accessible.

Acknowledgements

The authors express their gratitude to the staff and technician of the Laboratory of Biomolecules, Faculty of Science, Universitas Brawijaya, Indonesia, for their technical support. The authors also acknowledge appreciation to all those who provided valuable recommendations for this study, particularly Prof. Widodo, S.Si., Ph.D., M.Sc., who gave permission to utilize the Yasara software to investigate molecular dynamics on the computer in the molecular biology laboratory at Brawijaya University, Indonesia.

References

[1] SS Sundararaman, Y Doring and EPCVD Vorst. PCSK9: A multi-faceted protein that is involved in cardiovascular biology. *Biomedicines* 2021; **9(7)**, 793.

[2] K Fujisue and K Tsujita. Current status of lipid management in acute coronary syndrome. *Journal of Cardiology* 2017; **70(2)**, 101-106.

[3] EA Rosei and M Salvetti. Management of hypercholesterolemia, appropriateness of therapeutic approaches and new drugs in patients with high cardiovascular risk. *High Blood Pressure & Cardiovascular Prevention* 2016; **23**, 217-230.

[4] A Smith, D Johnson, J Banks, SW Keith and DG Karalis. Trends in PCSK9 inhibitor prescriptions before and after the price reduction in patients with atherosclerotic cardiovascular disease. *Journal of Clinical Medicine* 2021; **10(17)**, 3828.

[5] Y Handelsman and NE Lepor. PCSK9 inhibitors in lipid management of patients with diabetes mellitus and high cardiovascular risk: A review. *Journal of the American Heart Association* 2018; **7(13)**, e008953.

[6] Q Jia, H Cao, D Shen, S Li, L Yan, C Chen, S Xing and F Dou. Quercetin protects against atherosclerosis by regulating the expression of PCSK9, CD36, PPARγ, LXRα and ABCA1.

Internationnal Journal of Molecular Medicine 2019; **44(3)**, 893-902.

[7] M Mbikay, F Sirois, S Simoes, J Mayne and M Chretien. Quercetin-3-glucoside increases low-density lipoprotein receptor (LDLR) expression, attenuates proprotein convertase subtilisin/kexin 9 (PCSK9) secretion, and stimulates LDL uptake by Huh7 human hepatocytes in culture. *FEBS Open Bio* 2014; **4(1)**, 755-762.

[8] S Li, H Cao, D Shen, Q Jia, C Chen and SL Xing. Quercetin protects against ox-LDL-induced injury via regulation of ABCAl, LXR-α and PCSK9 in RAW264.7 macrophages. *Molecular Medicine Report* 2018; **18(1)**, 799-806.

[9] OJ Lara-Guzman, JH Tabares-Guevara, YM Leon-Varela, RM Alvarez, M Roldan, JA Sierra, JA Londono-Londono and JR Ramirez-Pineda. Proatherogenic macrophage activities are targeted by the flavonoid quercetin. *Journal of Pharmacology and Experimental Therapeutics November* 2012; **343(2)**, 296-306.

[10] S Egert, A Bosy-Westphal, J Seiberl, C Kurbitz, U Settler, S Plachta-Danielzik, AE Wagner, J Frank, J Schrezenmeir, G Rimbach, S Wolffram and MJ Muller. Quercetin reduces systolic blood pressure and plasma oxidised low-density lipoprotein concentrations in overweight subjects with a high-cardiovascular disease risk phenotype: a double-blinded, placebo-controlled cross-over study. *British Journal of Nutrition* 2009; **102**, 1065-1074.

[11] CS Wahono, MFR Syaban, MZ Pratama, PA Rahman and NE Erwan. Exploring the potential of phytoconstituents from Phaseolus vulgaris L against C-X-C motif chemokine receptor 4 (CXCR4): A bioinformatic and molecular dynamic simulations approach. *Egyptian Journal of Medical Human Genetics* 2024; **25**, 52.

[12] MSM Saleh, MJ Siddiqui, A Mediani, NH Ismail, QU Ahmed, SZM So'ad and S Saidi-Besbes. *Salacca zalacca*: A short review of the palm botany, pharmacological uses and phytochemistry. *Asian Pacific Journal of Tropical Medicine* 2018; **11(12)**, 645-652.

[13] E Girsang, INE Lister, CN Ginting, A Khu, B Samin, W Widowati, S Wibowo and R Rizal. Chemical constituents of snake fruit (Salacca zalacca (Gaert.) Voss) peel and *in silico* anti-aging analysis. *Molecular and Cellular Biomedical Sciences* 2019; **3(2)**, 122-128.

[14] LZ Benet, CM Hosey, O Ursu and TI Oprea. BDDCS, the rule of 5 and drugability. *Advanced Drug Delivery Reviews* 2016; **101**, 89-98.

[15] D Vijh and P Gupta. GC–MS analysis, molecular docking, and pharmacokinetic studies on dalbergia sissoo barks extracts for compounds with anti-diabetic potential. *Scientific Reports* 2024; **14**, 24936.

[16] AL Lomize, JM Hage, K Schnitzer, K Golobokov, MB LaFaive, AC Forsyth and ID Pogozheva. PerMM: A web tool and database for analysis of passive membrane permeability and translocation pathways of bioactive molecules. *Journal of Chemical Information and Modeling* 2019; **59(7)**, 3094-3099.

[17] DS Druzhilovskiy, AV Rudik, DA Filimonov, TA Gloriozova, AA Lagunin, AV Dmitriev, PV Pogodin, VI Dubovskaya, SM Ivanov, OA Tarasova, VM Bezhentsev, KA Murtazalieva, MI Semin, IS Maiorov, AS Gaur, GN Sastry and VV Poroikov. Computational platform Way2Drug: From the prediction of biological activity to drug repurposing. *Russian Chemical Bulletin* 2017; **66**, 1832-1841.

[18] SD Handari, MS Rohman, D Sargowo, Aulanni'am, RA Nugraha, B Lestari and D Oceandy. Novel impact of colchicine on interleukin-10 expression in acute myocardial infarction: An integrative approach. *Journal of Clinical Medicine* 2024; **13(16)**, 4619.

[19] WL Petrilli, GC Adam, RS Erdmann, P Abeywickrema, V Agnani, X Ai, J Baysarowich, N Byrne, JP Caldwell, W Chang, E DiNunzio, Z Feng, R Ford, S Ha, Y Huang, B Hubbard, JM Johnston, M Kavana, JM Lisnock, R Liang, …, JE Imbriglio. From screening to targeted degradation: Strategies for the discovery and optimization of small molecule ligands for PCSK9. *Cell Chemical Biology* 2020; **27(1)**, 32-40.

[20] BJ Oso, I Olaoye and OT Oso. Experimental and hypothetical appraisal on inhibition of glucose-induced glycation of bovine serum albumin by quercetin. *Journal of Genetic Engineering and Biotechnology* 2023; **21(1)**, 123.

[21] MH Widyananda, F Fatchiyah, L Muflikhah, SM Ulfa and N Widodo. Computational examination

to reveal Kaempferol as the most potent active compound from *Euphorbia hirta* against breast cancer by targeting AKT1 and ERα. *Egyptian Journal of Basic and Applied Sciences* 2023; **10(1)**, 753-767.

[22] K Kochl, T Schopper, V Durmaz, L Parigger, A Singh, A Krassnigg, M Cespugli, W Wu, X Yang, Y Zhang, WW Wang, C Selluski, T Zhao, X Zhang, C Bai, L Lin, Y Hu, Z Xie, Z Zhang, J Yan, …, CC Gruber. Optimizing variant-specific therapeutic SARS-CoV-2 decoys using deep-learning-guided molecular dynamics simulations. *Scientific Reports* 2023; **13**, 774.

[23] S Aralas, M Mohamed and MFA Bakar. Antioxidant properties of selected salak (*Salacca zalacca*) varieties in Sabah, Malaysia. *Nutrition & Food Science* 2009; **39(3)**, 243-250.

[24] NA Ismail and MFA Bakar. *Salak— Salacca zalacca*. Elsevier Science, Amsterdam, Netherlands, 2018.

[25] TH Simatupang, S Hartini, DA Mustika, A Purwoto, M Junef, A Sanusi, Firdaus, TWA Nugroho, J Mareta, A Jazuli and I Firdaus. Salak from indonesia: Legal protection, potential geographical indications and development practices toward international markets. *Cogent Social Sciences* 2024; **10(1)**, 2341963.

[26] MSM Saleh, MJ Siddiqui, HA Alshwyeh, NA Al-Mekhlafi, A Mediani, Z Ibrahim, NH Ismail and Y Kamisah. Metabolomics-based profiling with chemometric approach to identify bioactive compounds in Salacca zalacca fruits extracts and *in silico* molecular docking. *Arabian Journal of Chemistry* 2021; **14(4)**, 103038.

[27] NAM Zaini, A Osman, AA Hamid, A Ebrahimpour and N Saari. Purification and characterization of membrane-bound polyphenoloxidase (mPPO) from snake fruit [salacca zalacca (gaertn.) voss]. *Food Chemistry* 2013; **136(2)**, 407-414.

[28] M Marzuki, E Girsang, AN Nasution and INE Lister. Anti-diabetic effect of snake fruit skin extract in alloxan-induced wistar rat. *International Journal of Health and Pharmaceutical* 2022; **3(1)**, 146-153.

[29] M Kanlayavattanakul, N Lourith, D Ospondpant, U Ruktanonchai, S Pongpunyayuen and C Chansriniyom. Salak plum peel extract as a safe and efficient antioxidant appraisal for cosmetics. *Bioscience, Biotechnology, and Biochemistry* 2013; **77(5)**, 1068-1074.

[30] SS Tan, ST Tan and CX Tan. Antioxidant, hypoglycemic and anti-hypertensive properties of extracts derived from peel, fruit and kernel of *Salak*. *British Food Journal* 2020; **122(10)**, 3029-3038.

[31] R Roskoski. Properties of FDA-approved small molecule protein kinase inhibitors. *Pharmacological Research* 2019; **200**, 107059.

[32] SM Prijadi, S Aulia, A Afinasari, L Aristawidya, MDS Hikam and M Muchtaridi. *In silico* study of sesquiterpene and monoterpene compounds from valerian roots (valerian officinalis) as acetylcholinesterase inhibitor. *Indonesian Journal of Computational Biology* 2022; **1(1)**, 1-6.

[33] DSF Ramadhan, TM Fakih and A Arfan. Activity prediction of bioactive compounds contained in etlingera elatior against the SARS-CoV-2 main protease: An *in silico* approach. *Borneo Journal of Pharmacy* 2020; **3(4)**, 235-242.

[34] Fatimawali, TE Tallei, BJ Kepel, W Bodhi, AE Manampiring and F Nainu. Molecular Insight into the pharmacological potential of clerodendrum minahassae leaf extract for Type-2 diabetes management using the network pharmacology approach. *Medicina* 2023; **59(11)**, 1899.

[35] M Kulkarni, M Basanagouda, VB Jadhav and RN Rao. Computer aided prediction of biological activity spectra: Study of correlation between predicted and observed activities for Coumarin-4-Acetic acids. *Indian Journal of Pharmaceutical Sciences* 2011; **73(1)**, 88-92.

[36] H Cheng, N Xu, W Zhao, J Su, M Liang, Z Xie, X Wu and Q Li. (-)-Epicatechin regulates blood lipids and attenuates hepatic steatosis in rats fed high-fat diet. *Molecular Nutrition & Food Research* 2017; **61(11)**, 1700303.

[37] Y Yeh, Y Lee, H Hsieh and D Hwang. Dietary caffeic acid, ferulic acid and coumaric acid supplements on cholesterol metabolism and antioxidant activity in rats. *Journal of Food and Drug Analysis* 2020; **17(2)**, 123-132.

[38] Z Luo, M Li, J Yang, J Li, Y Zhang, F Liu, E El-Omar, L Han, J Bian, L Gong and M Wang. Ferulic acid attenuates high-fat diet-induced hypercholesterolemia by activating classic bile

acid synthesis pathway. *Frontiers in Nutrition* 2022; **9**, 976638.

[39] L Xiao, L Liu, X Guo, S Zhang, J Wang, F Zhou, L Liu, Y Tang and P Yao. Quercetin attenuates high fat diet-induced atherosclerosis in apolipoprotein E knockout mice: A critical role of NADPH oxidase. *Food and Chemical Toxicology* 2017; **105**, 22-33.

[40] H Yi, H Peng, X Wu, X Xu, T Kuang, J Zhang, L Du and G Fan. The therapeutic effects and mechanisms of quercetin on metabolic diseases: Pharmacological data and clinical evidence. *Oxidative Medicine and Cellular Longevity* 2021; **2021**, 6678662.

[41] Y Shao, Y Yu, C Li, J Yu, R Zong and C Pei. Synergistic effect of quercetin and 6-gingerol treatment in streptozotocin induced type 2 diabetic rats and poloxamer P-407 induced hyperlipidemia. *RSC Advances* 2016; **6(15)**, 12235-12242.

[42] A Rauf, M Imran, IA Khan, M Ur-Rehman, SA Gilani, Z Mehmood and MS Mubarak. Anticancer potential of quercetin: A comprehensive review. *Phytotherapy Research* 2018; **32(11)**, 2109-2130.

[43] RB Pingili, SR Challa, AK Pawar, V Toleti, T Kodali and S Koppula. A systematic review on hepatoprotective activity of quercetin against various drugs and toxic agents: Evidence from preclinical studies. *Phytotherapy Research* 2020; **31(1)**, 5-32.

[44] J Roslan, N Giribabu, K Karim and N Salleh. Quercetin ameliorates oxidative stress, inflammation and apoptosis in the heart of streptozotocin-nicotinamide-induced adult male diabetic rats. *Biomedicine & Pharmacotherapy* 2017; **86**, 570-582.

[45] E Tomou, P Papakyriakopoulou, E Saitani, G Valsami, N Pippa and H Skaltsa. Recent advances in nanoformulations for quercetin delivery. *Pharmaceutics* 2023; **15(6)**, 1656.

[46] V Venkatraman. FP-ADMET: A compendium of fingerprint-based ADMET prediction models. *Journal of Cheminformatics* 2021; **13**, 75.

[47] AS Setlur, C Karunakaran, V Panhalkar, S Sharma, M Sarkar and V Niranjan. Multifaceted computational profiling of thymol and geraniol against the human proteome for bio-repellent alternatives: Toxicity predictions, degradation analysis, and quantum mechanical approaches. *Acta Tropica* 2024; **258**, 107359.

[48] PC Agu, CA Afiukwa, OU Orji, EM Ezeh, IH Ofoke, CO Ogbu, EI Ugwuja and PM Aja. Molecular docking as a tool for the discovery of molecular targets of nutraceuticals in diseases management. *Scientific Reports* 2023; **13**, 13398.

[49] Y Yueniwati, MFR Syaban, IFD Faratisha, KC Yunita, DB Kurniawan, GFA Putra and NE Erwan. Molecular docking approach of natural compound from herbal medicine in java against severe acute respiratory syndrome coronavirus-2 Receptor. *Open Access Macedonian Journal of Medical Science* 2021; **9**, 1181-1186.

[50] Y Yueniwati, MFR Syaban, DB Kurniawan, AA Azam, DM Alvenia, YN Savira, RF Muhammad, B Adnani, AH Violita, SD Arviana, A Hasibuan, E Norahmawati, Y Fatmasari, A Mufidah, KA Savitri, UR Zulfikri, DY Putri and S Utami. 7,8-Dihydroxyflavone functions as an antioxidant through the inhibition of Kelch-like ECH-associated protein 1: Molecular docking and an *in vivo* approach in a rat model of ischemia-reperfusion brain injury. *World Academy of Sciences Journal* 2024; **6(2)**, 15.

[51] MFR Syaban, NE Erwan, MRR Syamsuddin, FA Zahra and FL Sabila. Molecular docking approach of viscosin as antibacterial for methicillin-resistant staphylococcus aureus Via Î²-Lactamase inhibitor mechanism. *Clinical and Research Journal in Internal Medicine* 2021; **2(2)**, 187-192.

[52] S Singh and VK Singh. *Molecular dynamics simulation: Methods and application.* Springer Nature, London, 2020.

[53] L Martinez. Automatic identification of mobile and rigid substructures in molecular dynamics simulations and fractional structural fluctuation analysis. *PLoS ONE* 2015; **10(3)**, e0119264.

[54] TL Wargasetia, H Ratnawati, N Widodo and MH Widyananda. Bioinformatics study of sea cucumber peptides as antibreast cancer through inhibiting the activity of overexpressed protein (EGFR, PI3K, AKT1, and CDK4). *Cancer Informatics* 2021; **20**, 11769351211031864.